Express Polymer Letters Vol.17, No.10 (2023) 1070–1080
Available online at www.expresspolymlett.com
https://doi.org/10.3144/expresspolymlett.2023.80

Research article

Kinetic studies on the transport behavior of hybrid filler incorporated natural rubber (NR)

Vakkoottil Sivadasan Abhisha[1], *Krishanagegham Sidharathan Sisanth*[2], *Sabu Thomas*[2,3], *Ranimol Stephen*[1*]

[1]Department of Chemistry, St. Joseph's College (Autonomous), Devagiri, Affiliated to University of Calicut, 673008 Calicut, Kerala, India
[2]International and Inter University Centre for Nanoscience and Nanotechnology (IIUCNN), Mahatma Gandhi University, P.D. Hills, 686560 Kottayam, Kerala, India
[3]School of Energy Materials, Mahatma Gandhi University, P.D. Hills, 686560 Kottayam, Kerala, India

Received 5 April 2023; accepted in revised form 11 July 2023

Abstract. Conductive carbon black (CCB), carbon nanotubes (CNT) and its hybrids are introduced into the natural rubber (NR) matrix aiming to explore the effect of filler ratio on the transport properties. Solvent transport of NR is found to decrease for hybrid filler systems as compared to single filler incorporated systems. Kinetic parameters of solvent transport behavior of filled NR systems are analyzed using various kinetic models. Upon the computation of kinetic parameters of transport data, it is found that the Peppas-Sahlin model is in good agreement with experimental observations, which suggests that the transport mechanism is diffusion controlled. Rubber–filler interaction parameters are computed and analyzed from the swelling experiments using Kraus, Cunneen-Russel, and Lorenz-Park equations.

Keywords: *crosslinking, curing, elastomer, filler, natural rubber, vulcanization, carbon black, transport properties*

1. Introduction

The role of polymer composites in the field of membrane technology demands a comprehensive understanding and in-depth knowledge of the transport behavior of solvents in the composite matrix. The transport properties of solvents in polymer composites are related to the distribution and reinforcement of fillers in the matrix. Polymer composites are widely used as food packaging materials owing to their intrinsic qualities such as corrosion resistance, lightweight, enhanced mechanical properties, and thermal properties [1]. Polymer composites containing chemically modified fillers empower the production of highly efficient membranes for pervaporation, ultrafiltration, reverse osmosis, and gas separation [2–8].

The solvent uptake of polymer composites depends on the characteristics of fillers, temperature, morphology, type of solvent, free volume, and processing conditions [9]. The transport of solvents in polymers is also affected by crosslink density, free volume, and structure of the polymer. Polymer chain segmental motions have a crucial influence on the processes associated with the diffusion of molecules through the polymer matrix. Variation in polymer composition and structure directly affects the free volume content and distribution, which in turn affects the transport of matter. The transport processes are interdependent with the polymeric structure and segmental motion of polymer chains [10].

Natural rubber (NR) based polymer composites are widely used in the automotive, construction, and electrical industries and for various engineering applications. Modification of the rubber matrix by the addition of various fillers generates interesting changes

*Corresponding author, e-mail: ranistephen@gmail.com

in the properties of composites, including transport properties. Carbonaceous fillers such as carbon nanotubes (CNT), graphene, carbon black (CB), carbon fibers, *etc.*, are extensively used fillers in NR. Among the carbon nanofillers, graphene and its derivatives can refine the barrier characteristics of elastomer composites. Graphene-loaded fluoroelastomer shows decreased swelling rates in acetone compared to CB-filled fluoroelastomer composite [11]. Similarly hybrid filler combination of graphene with zinc oxide in NR shows the capacity to resist chemical attack. The mol% uptake for hybrid filler composites shows a remarkable decrease of 41.7% for kerosene, 4.4% decrease for diesel, and 50% for polymethylsilane (PMS) and water, respectively, when compared to CB-filled NR as control [12]. CNT is commonly used as reinforcing fillers in NR due to its high strength and stiffness, exceptional electrical conductivity and high thermal conductivity, which can upgrade the properties of NR. The incorporation of a hybrid filler system is effective in restraining solvent penetration through the polymer matrix [13]. CNT/clay hybrid filler system improves the crosslink density of nitrile rubber (NBR)/NR blends [14]. Conductive carbon black (CCB), also known as electrically conductive black, is used as a reinforcement agent in the manufacture of electrical components such as electromagnetic interference (EMI) shielding shielding agents, static dissipative products and antistatic products [15–17].

The present study focuses on the solvent transport properties of single filler (CCB) and hybrid filler (CCB/CNT) reinforced NR composites as a function of filler concentration and its comparison. Experimentally obtained transport data are evaluated using different kinetic models such as first-order kinetics, Higuchi, Korsemayer-Peppas, and Peppas-Sahlin models. Theoretical understanding of the transport phenomena in rubber composites is beneficial in advanced research as well as in the fabrication of composite membranes. Empirical and semi-empirical mathematical models give a theoretical perspective of experimental transport data. This helps to elucidate the transport mechanism of solvents through the rubber matrix. Matrix-filler interactions are obtained from swelling studies and are evaluated using Kraus, Cunnen-Russel and Lorenz-Park plots. The combination of exploring a hybrid filler system, investigating the effects of filler ratio, applying kinetic modeling, and analyzing rubber-filler interactions contributes to the novelty and importance of the present study. The research gap in the reported work lies in the specific investigation of the synergistic effect of hybrid filler (CCB/CNT) on the transport properties of NR and its theoretical comparison as a function of filler concentration. This aspect has not been extensively studied before, and understanding the transport behavior in these composite systems is crucial for various applications in membrane technology.

2. Experimental

2.1. Materials

Natural rubber (NR) of grade ISNR 20 was purchased from the Rubber Research Institute of India (RRII), Kottayam, Kerala. All the compounding ingredients used were of commercial grade. Conductive carbon black (CCB) was provided by Continental Carbon India Limited (CCIL), Uttar Pradesh, India. The iodine number of CCB is 240±10 mg/g; Brunauer–Emmett–Teller surface area (BET) surface area is 260±10 m^2/g; ash content <0.60 wt% and density is 320±20 kg/m^3. Multiwall Carbon nanotubes (CNT) with ~99% purity were purchased from Adnano Technologies, India. CNT has a high aspect ratio; its diameter is ~5–15 nm, length ~10 μm, surface area ~260 m^2/g, and bulk density of 0.14 g/cm^3. Toluene obtained from Thermo Fisher Scientific Inc. (USA) (molecular weight: 92.14 g/mol, density: 0.866 g/cm^3 and solubility parameter 18.3 $MPa^{1/2}$) was employed for the diffusion studies of rubber composites.

2.2. Preparation of rubber composites

NR/CCB and NR/CCB/CNT composites were prepared by mixing NR and fillers in a Brabender plastograph for 8 min at 100 °C and 60 rpm. Amount of CCB is varied from 5 to 20 phr in NR/CCB composites and all NR/CCB/CNT composites contains 20 phr CCB. The amount of CNT is varied from 0.5 to 5 phr. Curatives were added in an open two-roll mill at room temperature for a total mixing time of 15 min. Preparation method of NR/CCB composites is reported in our previous work [18]. All the prepared NR composites contain 5 g – zinc oxide, 3 g – stearic acid, 1.3 g – *N*-cyclohexyl-2-benzothiazolesulfenamide (CBS), 0.1 g – 2-mercaptobenzothiazole (MBT), and 2.8 g sulfur corresponding to 100 phr NR. The samples were moulded in an electrically heated hydraulic press at 150 °C under a pressure of about 120 bar to the optimum cure time determined

from Moving Die Rheometer ASTM D5289. The NR/CCB samples are coded as NBx and NR/CCB/CNT samples are coded as NBxCy where 'N' represents natural rubber, 'B' represents conductive carbon black (CCB), 'x' represents the quantity of CCB [phr], 'C' represents carbon nanotubes (CNT), and 'y' represents the quantity of CNT [phr].

2.3. Characterization methods

2.3.1. Transport studies

The transport behavior of samples in toluene was studied at room temperature. Circular-shaped samples were immersed in 20 ml toluene and taken in closed diffusion bottles. The weight and thickness of the samples before immersing in a solvent were measured and recorded. The weight of the samples was taken in specific intervals until equilibrium swelling was reached. Each weighing was completed within 30 s to minimize the error due to the evaporation of solvent during weighing. The solvent uptake Q_t [%] of the samples was computed using the Equation (1) [19]:

$$Q_t = \frac{\frac{m_t - m_0}{M_S}}{m_0} \cdot 100 \quad (1)$$

where m_t is the mass of the sample at the time t of immersion and m_0 is the mass of the sample before immersion in the solvent. M_S is the molecular mass of solvent. Here, the molecular mass of toluene is 92.14 g/mol.

2.3.2. High-resolution transmission electron microscopy (HRTEM)

The distribution of CCB in the NR was analyzed through transmission electron microscopy (TEM) using JEOL-JEM 2100, Japan, and operated at 200 kV. The ultra-microtome (Leica, Ultracut UCT) was employed to crosscutting of specimens into ultrathin sections and sited on 300 mesh Cu grids at room temperature.

2.3.3. Swelling studies and crosslink density measurements

The swelling index indicates the swelling resistance of the rubber composites and is obtained using Equation (2) [20],

$$\text{Swelling index} = \frac{W_1 - W_0}{W_0} \cdot 100 \quad (2)$$

where W_1 and W_0 are the weight of the samples after swelling and before swelling in toluene. The swelling behavior of rubber composites can also be analyzed from the swelling coefficient value (α), which is an index of the ability with which the samples swell and is given by the Equation (3) [20]:

$$\alpha = \frac{W_\infty - W_0}{W_0} \cdot \frac{1}{\rho_S} \quad (3)$$

where W_∞ is the weight of the sample at equilibrium swelling in the solvent, W_0 is the weight of the samples before swelling and ρ_S is the density of the solvent used. Here density of toluene used is 0.866 g/cm^3.

The toluene swelling method defined in ASTMD-0471-16a was used to determine the crosslink densities of the samples. Circular-shaped samples are weighed and allowed to swell in toluene until equilibrium. Then after weighing, swelled samples are air-dried for 72 h to measure the de-swollen weight. The apparent crosslink density value is given by $1/Q$ where Q is the swell ratio and is given by Equation (4) [20]:

$$Q = \frac{W_1 - W_0}{W_0} \quad (4)$$

The actual crosslink density of the samples is calculated using the Flory-Rehner equation (Equation (5)) [20–23]:

$$\nu = \frac{\ln(1 - V_{rf}) + V_{rf} + \chi V_{rf}^2}{-2\rho_r V_s V_{rf}^{1/3}} \quad (5)$$

where V_{rf} is the volume fraction of rubber in the solvent-swollen filled sample, χ is the interaction parameter given by Equation (6) [24], ρ_r is the density of the polymer and V_s is the molar volume of solvent. Here molar volume of toluene is 106.3 cm^3/mol:

$$\chi = \beta + \frac{V_s}{RT}(\delta_p - \delta_s)^2 \quad (6)$$

where β is the lattice constant (0.34), R is the universal gas constant, T is the temperature, δ_p and δ_s are the solubility parameters of the polymer and solvent, respectively.

3. Results and discussion

3.1. Kinetic studies of transport properties

Transport properties of NR/CCB and NR-CCB/CNT systems are analyzed in toluene. The effect of filler on the solvent uptake of NR is depicted in Figures 1

and 2. Solvent absorption initially increases rapidly due to the solvent molecules' high concentration gradient in the NR matrix. Then the sorption approaches equilibrium, as indicated by the plateau region of the sorption curve. From Figure 1, it is clear that the solvent uptake of NR/CCB systems decreases significantly as a function of weight percentage of filler. This can be described in terms of the formation of filler-filler and matrix-filler networks, which hinder the diffusion of solvent molecules. The incorporation of hybrid filler further decreases the solvent uptake due to the increase in tortuosity of the diffusing path in the presence of CNT. Similar observations were found in the solvent transport behavior of the halloysite nanotubes-filled NR system [13]. A schematic illustration of the proposed hybrid filler network of CCB and CNT is given in Figure 3.

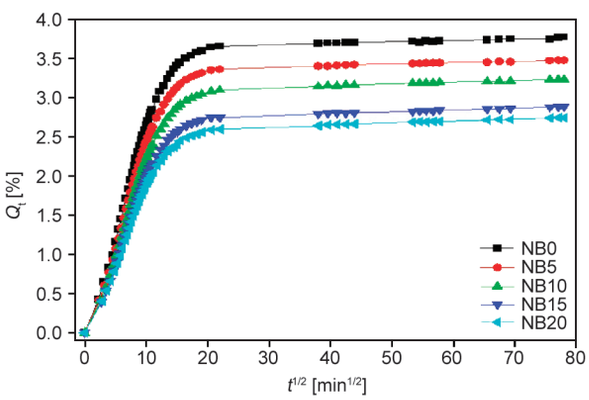

Figure 1. Sorption curves of NR/CCB systems.

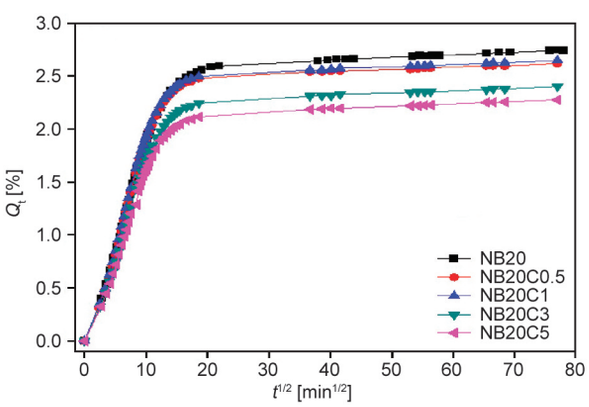

Figure 2. Sorption curves of NR/CCB/CNT systems.

The diffusion coefficient and permeability coefficient values of the CCB and CCB/CNT loaded systems are given in Table 1. The diffusion coefficient is calculated from the equation derived from the second Fickian law (Equation (7)) [25–28]:

$$D = \pi\left(\frac{h\theta}{4Q_\infty}\right)^2 \tag{7}$$

where h is the thickness of the sample, θ is the slope of the initial linear portion of the plot of Q_t [%] against $t^{1/2}$, and Q_∞ the equilibrium absorption. The diffusion coefficient gives the diffusion rate of solvent molecules into the polymer matrix. The diffusion coefficient value decreases linearly with filler loading. Polymer-filler interaction has decreased the availability of free voids, thereby restricting solvent diffusion through the matrix.

The permeability coefficient (P) of toluene in the NR/CCB and NR/CCB/CNT composites is given by Equation (8) [29]:

$$P = D \cdot S \tag{8}$$

where D is the diffusion coefficient and S is the sorption coefficient. The sorption coefficient is calculated from the Equation (9) [24]:

$$S = \frac{m_\infty}{m_0} \tag{9}$$

where m_∞ is the mass of the solvent absorbed at equilibrium and m_0 is the mass of the sample before immersion in the solvent. Sorption involves the initial penetration of solvent molecules and their dispersion across the rubber matrix [30] So, the sorption coefficient depends on the solvent-rubber interaction. The permeability coefficient has both contributions from diffusion and sorption. Decreasing the permeation coefficient with filler loading also suggests improved

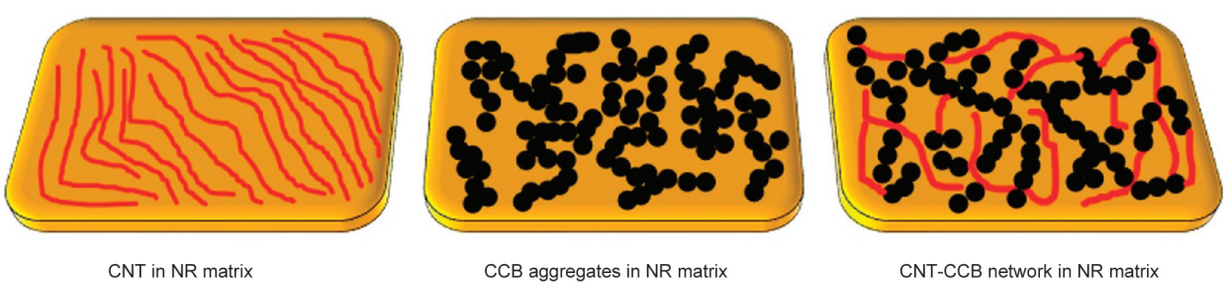

Figure 3. Schematic illustration of hybrid filler network of CCB and CNT.

Table 1. Diffusion coefficient and permeability coefficient.

Sample	$D \cdot 10^{-6}$ [cm^2/s]	$P \cdot 10^{-6}$ [cm^2/s]
NB0	2.14	7.45
NB5	1.96	6.29
NB10	1.74	5.18
NB15	1.45	3.86
NB20	1.22	3.08
NB20C0.5	1.16	2.79
NB20C1	1.10	2.66
NB20C3	1.01	2.23
NB20C5	0.90	1.88

filler-matrix interaction with increasing CCB and hybrid filler content. The permeation coefficient is decreased further upon the introduction of CNT to the single filler system. The interaction of filler and rubber restricts solvent swelling by the formation of crosslinks, which in turn, reduces the segmental mobility of rubber chains. Decreased flexibility of the chains as well as the reduction in the number of voids in the matrix, provides a hindrance to the diffusion of solvent molecules.

The mode of transport is analyzed using Equation (10):

$$\log \frac{Q_t}{Q_\infty} = \log k + n \log t \tag{10}$$

where Q_t is the solvent uptake at time t and Q_∞ is the equilibrium solvent uptake. The constants n and k are determined from the linear portion of the plot Q_t *versus* $t^{1/2}$ (Figures 1 and 2) through power regression analysis. The value of k depends upon the structural characteristics of polymer and polymer-solvent interaction, and n indicates the transport mechanism. The n values are computed (Table 2) and are in between 0.5 and 1 for all composites indicating the non-Fickian mode of transport [20, 27, 31, 32]. For the non-Fickian mode, the chain relaxation is much slower than the solvent penetration. A high degree of restriction produced by the filler particles reduces the segmental mobility of the rubber matrix [33]. Thus, the polymer matrix requires more time for rubber chain rearrangement in response to swelling stress to accommodate solvent molecules. Moreover, incorporated CCB particles diffuse into the cross-linked polymer chains and restrict the chain relaxation.

Table 2. Constant n indicating transport mechanism.

Sample	*n*
NB0	0.62
NB5	0.62
NB10	0.63
NB15	0.64
NB20	0.61
NB20C0.5	0.62
NB20C1	0.62
NB20C3	0.62
NB20C5	0.62

Theoretical computation is performed on the experimental solvent uptake properties of NR-filler system to attain a better understanding of the mode of transport in composites. We have employed first-order kinetics, Higuchi, Korsemayer-Peppas, and Peppas-Sahlin models to evaluate the transport properties. The first-order kinetic equation is given as (Equation (11) [27]:

$$\log Q_t = \log Q_\infty - \frac{kt}{2.303} \tag{11}$$

where Q_t is the solvent uptake at time t, Q_∞ is the equilibrium solvent uptake, k is the first-order rate constant. The correlation coefficient (R^2) obtained suggests that solvent diffusion in NR/CCB and NR/CCB/CNT composites does not follow first-order kinetics. Higuchi's model proposed that diffusion is based on Fick's law and also it depends on the square root of time. This model is based on the following hypothesis: (a) diffusion is one dimensional, (b) the diffusing particles are much smaller than matrix systems, (c) diffusivity is a constant and (d) matrix swelling and diffusion are constant [34] Higuchi model is simplified as Equation (12):

$$\frac{Q_t}{Q_\infty} = k_h t^{1/2} \tag{12}$$

where k_h is the Higuchi dissolution constant, t is the time and Q_t is the solvent uptake. Higuchi dissolution constant decreased linearly with an increase in filler loadings. Korsemeyer-Peppas [35] model helps to analyze the transport mechanism by the exponential Equation (13):

$$\frac{Q_t}{Q_\infty} = kt^n \tag{13}$$

where k is the kinetic constant, n is the diffusional exponent that indicates the transport mechanism.

Peppas-Sahlin model is based on the theory that the transport mechanism has diffusional and relaxational

contributions, which are additive in nature [36]. Peppas-Sahlin equation is given by Equation (14) [37]:

$$\frac{M_t}{M_\infty} = k_1 t^m + k_2 t^{2m} \quad (14)$$

where first term of the right-hand side is the Fickian contribution, the second term is the case-II relaxational contribution and m is the purely Fickian diffusion exponent for a device of any geometrical shape that exhibits controlled release. Previous works on transport mechanisms of polymeric systems have shown that $k_1 > k_2$ implies a diffusion-controlled mechanism, $k_1 < k_2$ implies a matrix-controlled mechanism, and $k_1 = k_2$ implies a combination of diffusion-controlled and matrix-controlled mechanisms [19]. Constants of various kinetic models are given in Table 3. Peppas-Sahlin model fits well for the solvent diffusion of NR/CCB and NR/CCB/CNT composites. In Peppas-Sahlin theoretical prediction, the k_1 values of all compositions are greater than k_2. The constant k_1 decreases with CB addition up to 15 phr. NB20 has k_1 value higher than NB0. CNT-incorporated composites have almost similar k_1 values. The constant values obtained suggest diffusion controlled transport mechanism in all samples. Fickian diffusion of solvent molecules in the composites is driven by the chemical potential gradient. Theoretical predictions of solvent permeation of NB20 using Higuchi, Korsemayer-Peppas and Peppas-Sahlin are depicted in Figure 4.

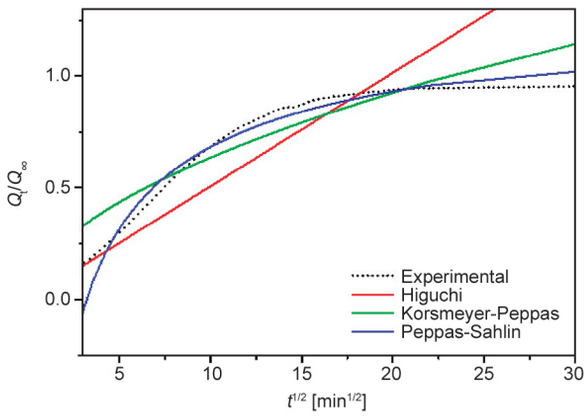

Figure 4. Model fitting of solvent permeation of NB20 using Higuchi, Korsmeyer-Peppas and Peppas-Sahlin equations.

3.2. Theoretical prediction of rubber-filler interaction from swelling studies

The extent of interaction between rubber and CCB and CCB/CNT can be analyzed using Kraus [38], Cunneen and Russel [39] and Lorenz and Park [40] equations. Kraus equation is (Equation (15)):

$$\frac{V_{r0}}{V_{rf}} = 1 - m\frac{f}{1-f} \quad (15)$$

where V_{r0} is the volume fraction of rubber in the solvent-swollen gum vulcanizate, m is the polymer-filler interaction parameter, f is the volume fraction of filler, and V_{rf} is the volume fraction of rubber in the solvent-swollen filled vulcanizate and is given by the Ellis and Welding equation (Equation (16)) [41]:

$$V_{rf} = \frac{\frac{d - f\cdot W}{\rho_p}}{\frac{d - f\cdot W}{\rho_p} + \frac{A_S}{\rho_S}} \quad (16)$$

where d is the non-swollen weight of the sample, f is the weight fraction of filler, W is the initial weight of sample, ρ_p is the density of polymer, ρ_S is the density of solvent and A_S is the amount of solvent absorbed. Plot of V_{r0}/V_{rf} against $f/(1-f)$ gives a straight line whose slope m gives the direct measure of reinforcement by CCB and CCB/CNT. According to Kraus model, reinforcing fillers will have a negative slope [42–44]. V_{r0}/V_{rf} represents the extent of swelling

Table 3. Correlation coefficients and constants of various kinetic models.

Sample		NB0	NB5	NB10	NB15	NB20	NB20C0.5	NB20C1	NB20C3	NB20C5
First order kinetics	k	0.0136	0.0134	0.0132	0.0163	0.0155	0.0156	0.0151	0.0148	0.0146
	R^2	0.8287	0.8390	0.8814	0.8861	0.8907	0.8595	0.8621	0.8766	0.8727
Higuchi model	k_h	0.0519	0.0518	0.0511	0.0512	0.0508	0.0293	0.0293	0.0290	0.0291
	R^2	0.8236	0.8226	0.8255	0.8201	0.8216	0.9595	0.9656	0.9691	0.9523
Korsemayer-Peppas model	k	0.1824	0.1814	0.1759	0.1807	0.1820	0.2189	0.2240	0.1544	0.1546
	n	0.2753	0.2760	0.2790	0.2745	0.2716	0.2379	0.2341	0.2716	0.2716
	R^2	0.9741	0.9878	0.9879	0.9864	0.9714	0.9846	0.9833	0.9863	0.9808
Peppas-Sahlin model	k_1	19.7668	13.3063	12.6867	11.5134	19.8209	19.7565	19.7498	19.7363	19.9999
	k_2	–20.2244	–13.8480	–13.1724	–12.0388	–20.3471	–20.2367	–20.2425	–20.2549	–20.0001
	m	–0.0131	–0.0214	–0.0211	–0.0242	–0.0137	–0.0136	–0.0138	–0.0139	–0.0046
	R^2	0.9821	0.9816	0.9829	0.9847	0.9891	0.9844	0.9868	0.9872	0.9864

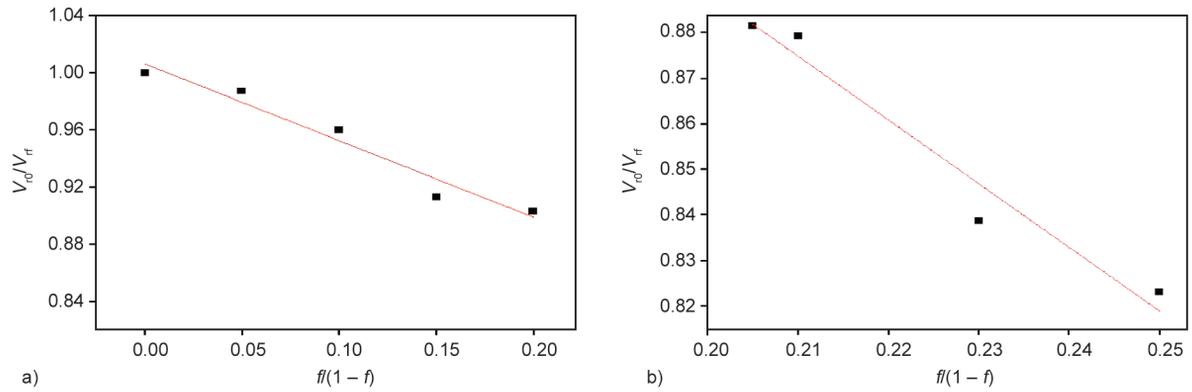

Figure 5. Kraus plots: a) NR/CCB systems b) NR/CCB/CNT systems.

restriction of the rubber matrix owing to the presence of incorporated filler. Kraus plots are given in Figures 5. Here, as the CCB loading increases the solvent uptake of the samples decreases (Figure 5a). Consequently, the V_{rf} values increase, leading to decreases in V_{r0}/V_{rf} values with the filler loading of CCB. Kraus plot gives a negative slope signifying the reinforcement effect of CCB on the rubber matrix. Kraus plot of NR/CCB/CNT systems also gives a negative slope suggesting the synergistic effect of the hybrid filler system on NR matrix. Well-dispersed CCB aggregates and hybrid filler networks of CCB and CNT create stronger interfaces in NR matrix. This leads to the restriction of solvent absorption in the NR.

Cunneen-Russel equation is Equation (17) [22]:

$$\frac{V_{r0}}{V_{rf}} = a\,e^{-z} + b \tag{17}$$

Plot of V_{r0}/V_{rf} against e^{-z}, where z is the weight fraction of filler, gives a straight line with slope a and intercept b. The cunneen-Russel plot of NR/CCB and NR/CCB/CNT composites is given in Figure 6. A positive slope indicates the reinforcement effect of filler on the rubber matrix. Incorporating CCB and hybrid fillers renders a positive slope of the Cunneen-Russel plot, which again supports the fact that the filler effectively interacts with the rubber matrix [22].

Lorenz and Parks equation is Equation (18) [45]:

$$\frac{Q_f}{Q_g} = a\,e^{-z} + b \tag{18}$$

where Q is the amount of solvent imbibed per unit weight, f and g refer to filled and gum rubber vulcanizates, a and b are the constants that depend on the filler activity and z is the weight fraction of filler in the rubber composites. The Q_f/Q_g values indicate the rubber-filler interaction. Decrease in Q_f/Q_g with filler loading signifies a greater extent of filler-matrix interaction. Lorenz and Parks plot of NR/CCB and NR/CCB/CNT composites is given in Figure 7. Plot of Q_f/Q_g against e^{-z} gives a straight line with a positive slope of 1.9267 and y-intercept of –0.9116 for NR/CCB composites. NR/CCB/CNT composites yield a positive slope of 3.6423 and y-intercept of –2.3649. A higher value of constant a and lower

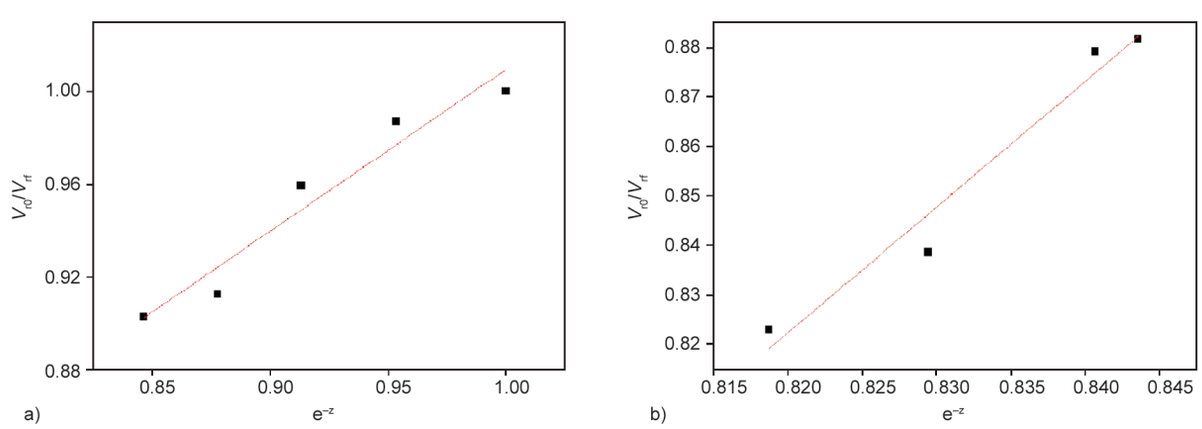

Figure 6. Cunneen-Russel plots; a) NR/CCB systems b) NR/CCB/CNT systems.

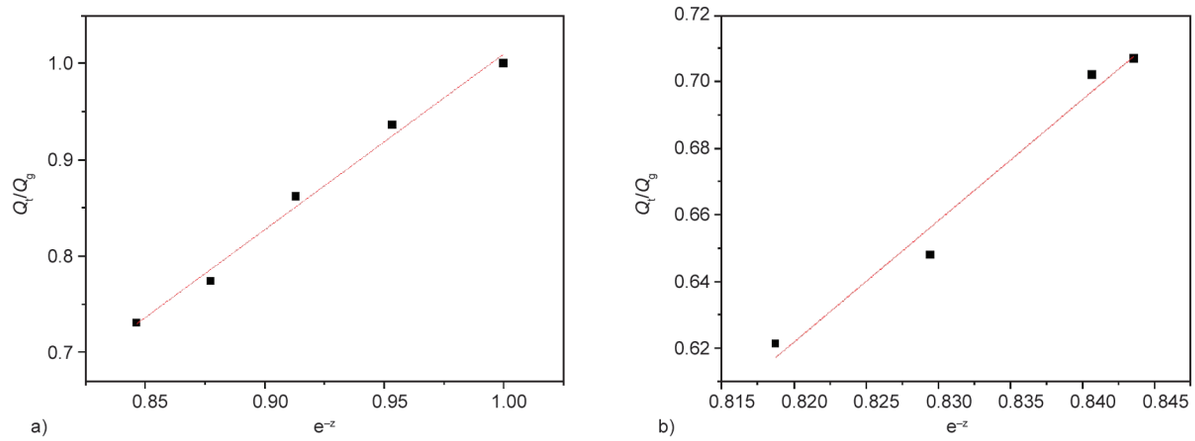

Figure 7. Lorenz-Park plots; a) NR/CCB systems b) NR/CCB/CNT systems.

value of constant b indicates the extent of polymer-filler interaction [45]. The value of constant '*a*' increased for hybrid filler incorporated NR than single filler system, suggesting the enhanced polymer-filler interaction for hybrid system. Higher difference between constant values '*a*' and '*b*' point towards the distinguished filler- rubber interaction.

The morphology of the hybrid filler system is evaluated using TEM. TEM images of the NB20, NB20C3 and NB20C5 is given in Figure 8. CCB aggregates in the matrix are linked together to form a filler network across the matrix in NB20 and some voids can also be present in the matrix (Figure 8a). Extensive filler network formation of CNT and spherical CCB particles are seen when 3 phr of CNT is added to 20 phr CCB (Figure 8b). CNT and CCB particles are uniformly dispersed in the rubber matrix. A similar morphology is observed for NB20C5 also, but voids observed are less when compared to NB20C3 (Figure 8c). Effective filler network formation and uniform dispersion of fillers can be explained in terms of the combination of two processing techniques employed for compounding. Morphological data support the previous results of Kraus, Cunnen-Russel and Lorenz-Park analysis of swelling studies.

3.3. Swelling index and crosslink density

The swelling index and swelling coefficient of NR/CCB and NR/CCB/CNT composites are presented in Table 4. Both swelling index [%] and swelling coefficient decrease linearly with filler loading increase, indicating the restriction of swelling in the filled composites. Hybrid filler network formation restricts the movement of solvent particles through

Table 4. Swelling index [%] and swelling coefficient.

Sample	Swelling index [%]	Swelling coefficient
NB0	339.6	3.92
NB5	317.9	3.67
NB10	292.8	3.38
NB15	262.8	3.03
NB20	248.2	2.86
NB20C0.5	240.1	2.77
NB20C1	238.4	2.75
NB20C3	220.0	2.54
NB20C5	211.0	2.43

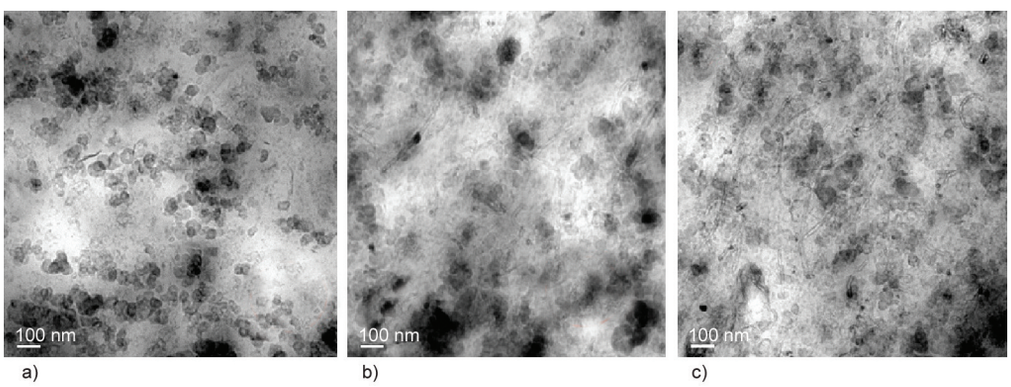

Figure 8. TEM images; a) CCB aggregates in NB20; CNT/CCB network in b) NB20C3 and c) NB20C5.

the polymer matrix. Swelling values gives an insight into the crosslink density of samples. CCB and CNT fillers occupy the free volume of NR matrix resulting in a decrease in the voids in the rubber matrix. The incorporation of fillers offers a tortuous path for diffusing solvent molecules. Thus, the solvent uptake of the filled composites decreases.

The extent of crosslinking can be deducted from the V_{rf} values of the composites. Table 5 shows the V_{rf} values of the NR/CCB and NR/CCB/CNT composites. V_{rf} values are gradually increasing with the filler loading, pointing towards the better interaction of rubber-filler and the formation of crosslinks. Apparent crosslink density values given by $1/Q$ in Table 5 also support the same.

The crosslink density of the NR/CCB and NR/CCB/CNT composites is constantly increasing with filler loading (Table 5). It further supports the reinforcement effect of CCB on NR matrix and the synergistic effect of hybrid filler as well. The values of crosslink density indicate the physical and chemical crosslinks in the system, such as sulfidic linkages, filler-filler and filler-rubber interactions [46].

4. Conclusions

Incorporating hybrid filler consisting of CCB and CNT in NR composites leads to forming a filler network that enhances the transport properties of the composites. The hybrid filler system exhibits increased crosslink density and reduced diffusion coefficient compared to composites containing a single filler. Crosslink density of NR increased significantly upon the addition of 20 phr of CCB. Moreover, the addition of 5 phr CNT along with 20 phr CCB further enhanced the crosslink density, thereby reducing the diffusion coefficient by around 42% when compared to neat NR. Theoretical models were applied to the diffusion data for a better understanding of the transport mechanism. The morphological characterization and theoretical analysis confirm the rubber-filler network formation in NR/hybrid filler systems. Hybrid filler NR composites demonstrate superior transport characteristics compared to composites with single fillers.

Table 5. Volume fraction of rubber (V_{rf}), apparent crosslink density ($1/Q$) and crosslinkdensity (ν) of materials.

Sample	V_{rf}	$1/Q$	ν [g/mol/cm^3]
NB0	0.2119	0.29	$7.28 \cdot 10^{-5}$
NB5	0.2147	0.31	$7.49 \cdot 10^{-5}$
NB10	0.2208	0.34	$7.98 \cdot 10^{-5}$
NB15	0.2322	0.38	$8.91 \cdot 10^{-5}$
NB20	0.2347	0.40	$9.14 \cdot 10^{-5}$
NB20C0.5	0.2404	0.42	$9.64 \cdot 10^{-5}$
NB20C1	0.2410	0.42	$9.70 \cdot 10^{-5}$
NB20C3	0.2527	0.45	$1.08 \cdot 10^{-4}$

Acknowledgements

One of the authors, V. S. Abhisha is thankful to University Grants Commission (UGC), New Delhi for the UGC-JRF fellowship. Also, the first and corresponding authors are thankful to Rashtriya Uchchatar Shiksha Abhiyan (RUSA), New Delhi, India for the financial support.

References

[1] Zhang M., Biesold G. M., Choi W., Yu J., Deng Y., Silvestre C., Lin Z.: Recent advances in polymers and polymer composites for food packaging. Materials Today, **53**, 134–161 (2022). https://doi.org/10.1016/j.mattod.2022.01.022

[2] Swapna V. P., Jose T., George S. C., Thomas S., Stephen R.: Pervaporation separation of an azeotropic mixture of a tetrahydrofuran–water system with nanostructured polyhedral oligomeric silsesquioxane embedded poly (vinyl alcohol). Journal of Applied Polymer Science, **136**, 47060 (2019). https://doi.org/10.1002/app.47060

[3] Swapna V. P., Thomas S. P., Jose T., Moni G., George S. C., Thomas S., Stephen R.: Mechanical properties and pervaporation separation performance of CTAB-modified cage-structured POSS-incorporated PVA membrane. Journal of Materials Science, **54**, 8319–8331 (2019). https://doi.org/10.1007/s10853-019-03479-8

[4] Swapna V. P., Nambissan P. M. G., Thomas S. P., Vayyaprontavida Kaliyathan A., Jose T., George S. C., Thomas S., Stephen R.: Free volume defects and transport properties of mechanically stable polyhedral oligomeric silsesquioxane embedded poly(vinyl alcohol)-poly(ethylene oxide) blend membranes. Polymer International, **68**, 1280–1291 (2019). https://doi.org/10.1002/pi.5815

[5] Swapna V. P., Kaliyathan A. V., Abhisha V. S., Maria H. J., Nambissan P. M. G., Thomas S., Stephen R.: Changes in free volume and gas permeation properties of poly(vinyl alcohol) nanocomposite membranes modified using cage-structured polyhedral oligomeric silsesquioxane. Journal of Applied Polymer Science, **138**, 49953 (2021). https://doi.org/10.1002/app.49953

[6] Stephen R., Joseph K., Oommen Z., Thomas S.: Molecular transport of aromatic solvents through microcomposites of natural rubber (NR), carboxylated styrene butadiene rubber (XSBR) and their blends. Composites Science and Technology, **67**, 1187–1194 (2007). https://doi.org/10.1016/j.compscitech.2006.05.009

[7] Thomas S., George S. C., Jose T.: Polymer nanocomposite membranes for pervaporation. Elsevier, Amsterdam (2020).

[8] Li D., Yan Y., Wang H.: Recent advances in polymer and polymer composite membranes for reverse and forward osmosis processes. Topical Volume on Polymer Hybrid Materials, **61**, 104–155 (2016). https://doi.org/10.1016/j.progpolymsci.2016.03.003

[9] Thomas S., Wilson R., Anil Kumar S., George S. C.: Transport properties of polymeric membranes. Elsevier, Amsterdam (2017).

[10] Rogers C. E., Semancik J. R., Kapur S.: Transport processes in polymers. in 'Structure and properties of polymer films: Based upon the borden award symposium in honor of Richard S. Stein' (eds.: Lenz R. W., Stein R. S.) Springer, Boston, 297–319 (1973).

[11] Liu M., Cataldi P., Young R. J., Papageorgiou D. G., Kinloch I. A.: High-performance fluoroelastomer-graphene nanocomposites for advanced sealing applications. Composites Science and Technology, **202**, 108592 (2021). https://doi.org/10.1016/j.compscitech.2020.108592

[12] Ekebafe L., Nworie E. C., Mahmud H.: Mechanical and sorption indices of ZnO-rGO hybrid filled natural rubber nanocomposites. Journal of Scientific Research and Development, **20**, 209–224 (2021).

[13] Abhisha V. S., Augustine A., Joseph J., Thomas S. P., Stephen R.: Effect of halloysite nanotubes and organically modified bentonite clay hybrid filler system on the properties of natural rubber. Journal of Elastomers and Plastics, **52**, 432–452 (2020). https://doi.org/10.1177/0095244319865573

[14] Thomas S., Abraham J., George S. C., Thomas S.: Role of CNT/clay hybrid on the mechanical, electrical and transport properties of NBR/NR blends. Polymer Bulletin, **77**, 1–16 (2020). https://doi.org/10.1007/s00289-019-02693-3

[15] Cheng H., Cao C., Zhang Q., Wang Y., Liu Y., Huang B., Sun X-L., Guo Y., Xiao L., Chen Q.: Enhancement of electromagnetic interference shielding performance and wear resistance of the UHMWPE/PP blend by constructing a segregated hybrid conductive carbon black–polymer network. ACS Omega, **6**, 15078–15088 (2021). https://doi.org/10.1021/acsomega.1c01240

[16] Jia L. J., Phule A. D., Geng Y., Wen S., Li L., Zhang Z. X.: Microcellular conductive carbon black or graphene/PVDF composite foam with 3D conductive channel: A promising lightweight, heat-insulating, and EMI-shielding material. Macromolecular Materials and Engineering, **306**, 2000759 (2021). https://doi.org/10.1002/mame.202000759

[17] da Silva T. F., Menezes F., Montagna L. S., Lemes A. P., Passador F. R.: Preparation and characterization of antistatic packaging for electronic components based on poly(lactic acid)/carbon black composites. Journal of Applied Polymer Science, **136**, 47273 (2019). https://doi.org/10.1002/app.47273

[18] Abhisha V. S., Sisanth K. S., Parameswaranpillai J., Pulikkalparambil H., Siengchin S., Thomas S., Stephen R.: Comprehensive experimental investigations and theoretical predictions on the physical properties of natural rubber composites. Journal of Applied Polymer Science, **139**, e53197 (2022). https://doi.org/10.1002/app.53197

[19] Zachariah A. K., Kumar Chandra A., Mohamed P. K., Parameswaranpillai J., Thomas S.: Mixed mode morphology in elastomeric blend nanocomposites: Effect on vulcanization, thermal stability and solvent permeability. Polymer Composites, **39**, E1659–E1668 (2018). https://doi.org/10.1002/pc.24624

[20] Kaliyathan A. V., Rane A. V., Jackson S., Thomas S.: Analysis of diffusion characteristics for aromatic solvents through carbon black filled natural rubber/butadiene rubber blends. Polymer Composites, **42**, 375–396 (2021). https://doi.org/10.1002/pc.25832

[21] Flory P. J., Rehner J.: Statistical mechanics of cross-linked polymer networks II. Swelling. Journal of Chemical Physics, **11**, 521–525 (1943). https://doi.org/10.1063/1.1723792

[22] Swapna V. P., Stephen R., Greeshma T., Sharan Dev C., Sreekala M. S.: Mechanical and swelling behavior of green nanocomposites of natural rubber latex and tubular shaped halloysite nano clay. Polymer Composites, **37**, 602–611 (2016). https://doi.org/10.1002/pc.23217

[23] Abraham J., Sidhardhan Sisanth K., Zachariah A. K., Mariya H. J., George S. C., Kalarikkal N., Thomas S.: Transport and solvent sensing characteristics of styrene butadiene rubber nanocomposites containing imidazolium ionic liquid modified carbon nanotubes. Journal of Applied Polymer Science, **137**, 49429 (2020). https://doi.org/10.1002/app.49429

[24] James J., Thomas G. V., Pramoda K. P., Thomas S.: Transport behaviour of aromatic solvents through styrene butadiene rubber/poly[methyl methacrylate] (SBR/PMMMA) interpenetrating polymer network (IPN) membranes. Polymer, **116**, 76–88 (2017). https://doi.org/10.1016/j.polymer.2017.03.063

[25] Stephen R., Thomas S., Raju K. V. S. N., Varghese S., Joseph K., Oommen Z.: Dynamic mechanical and dielectric properties of nanocomposites of natural rubber (NR), carboxylated styrene butadiene rubber (XSBR) latices and their blends. Rubber Chemistry and Technology, **80**, 672–689 (2007). https://doi.org/10.5254/1.3548187

[26] Stephen R., Varghese S., Joseph K., Oommen Z., Thomas S.: Diffusion and transport through nanocomposites of natural rubber (NR), carboxylated styrene butadiene rubber (XSBR) and their blends. Journal of Membrane Science, **282**, 162–170 (2006). https://doi.org/10.1016/j.memsci.2006.05.019

[27] Maria H. J., Lyczko N., Nzihou A., Mathew C., George S. C., Joseph K., Thomas S.: Transport of organic solvents through natural rubber/nitrile rubber/organically modified montmorillonite nanocomposites. Journal of Materials Science, **48**, 5373–5386 (2013). https://doi.org/10.1007/s10853-013-7332-7

[28] Abraham J., Maria H. J., George S. C., Kalarikkal N., Thomas S.: Transport characteristics of organic solvents through carbon nanotube filled styrene butadiene rubber nanocomposites: The influence of rubber-filler interaction, the degree of reinforcement and morphology. Physical Chemistry Chemical Physics, **17**, 11217–11228 (2015). https://doi.org/10.1039/c5cp00719d

[29] Arani A. G., Jafari G. S., Kolahchi R.: Vibration analysis of nanocomposite microplates integrated with sensor and actuator layers using surface SSDPT. Polymer Composites, **39**, 1936–1949 (2016). https://doi.org/10.1002/pc.24150

[30] Danwanichakul P., Jaroenkarn S., Jumpathi P., Dechojarassri D.: Sorption and desorption of toluene, *m*-xylene, *p*-cresol and water by natural rubber chips. Songklanakarin Journal of Science and Technology, **28**, 1071–1082 (2006).

[31] Igwe I. O., Ezeani O. E.: Studies on the transport of aromatic solvents through filled natural rubber. International Journal of Polymer Science, **2012**, 212507 (2012). https://doi.org/10.1155/2012/212507

[32] Thimmaiah S. R., Siddaramaiah: Diffusion and transport behaviors of aliphatic probe molecules through untreated and treated metakaolin filled natural rubber composites. Applied Polymer Composites, **1**, 247 (2013).

[33] Therattil J., Anil Kumar S.: Transport of organic solvents through ionic liquid modified natural rubber/MWCNT composites. International Journal of Scientific and Technology Research, **9**, 3055–3064 (2020).

[34] Sambhudevan S., Shankar B., Appukuttan S., Joseph K.: Evaluation of kinetics and transport mechanism of solvents through natural rubber composites containing organically modified gadolinium oxide. Plastics, Rubber and Composites, **45**, 216–223 (2016). https://doi.org/10.1080/14658011.2016.1165904

[35] Korsmeyer R. W., Gurny R., Doelker E., Buri P., Peppas N. A.: Mechanisms of solute release from porous hydrophilic polymers. International Journal of Pharmaceutics, **15**, 25–35 (1983). https://doi.org/10.1016/0378-5173(83)90064-9

[36] Jose J. P., Thomas S.: XLPE based Al_2O_3–clay binary and ternary hybrid nanocomposites: Self-assembly of nanoscale hybrid fillers, polymer chain confinement and transport characteristics. Physical Chemistry Chemical Physics, **16**, 20190–20201 (2014). https://doi.org/10.1039/C4CP03403A

[37] Peppas N. A., Sahlim J. J.: A simple equation for the description of solute release. III. Coupling of diffusion and relaxation. International Journal of Pharmaceutics, **57**, 169–172 (1989). https://doi.org/10.1016/0378-5173(89)90306-2

[38] Kraus G.: Swelling of filler-reinforced vulcanizates. Journal of Applied Polymer Science, **7**, 861–871 (1963). https://doi.org/10.1002/app.1963.070070306

[39] Cunneen J. I., Russell R. M.: Occurrence and prevention of changes in the chemical structure of natural rubber tire tread vulcanizates during service. Rubber Chemistry and Technology, **43**, 1215–1224 (1970). https://doi.org/10.5254/1.3547319

[40] Lorenz O., Parks C. R.: The crosslinking efficiency of some vulcanizing agents in natural rubber. Journal of Polymer Science, **50**, 299–312 (1961). https://doi.org/10.1002/pol.1961.1205015404

[41] Ellis B., Welding G. N.: Estimation, from swelling, of the structural contribution of chemical reactions to the vulcanization of natural rubber. Part II. Estimation of equilibrium degree of swelling. Rubber Chemistry and Technology, **37**, 571–575 (1964). https://doi.org/10.5254/1.3540349

[42] Stephen R., Alex R., Cherian T., Varghese S., Joseph K., Thomas S.: Rheological behavior of nanocomposites of natural rubber and carboxylated styrene butadiene rubber latices and their blends. Journal of Applied Polymer Science, **101**, 2355–2362 (2006). https://doi.org/10.1002/app.23852

[43] Thomas S., George S., Thomas S.: Rigid amorphous phase: Mechanical and transport properties of nitrile rubber/clay nanocomposites. Progress in Rubber, Plastics and Recycling Technology, **33**, 103–126 (2017). https://doi.org/10.1177/147776061703300204

[44] Gobetti A., Cornacchia G., la Monica M., Zacco A., Depero L. E., Ramorino G.: Assessment of the influence of electric arc furnace slag as a non-conventional filler for nitrile butadiene rubber. Results in Engineering, **17**, 100987 (2023). https://doi.org/10.1016/j.rineng.2023.100987

[45] Zachariah A. K., Chandra A. K., Mohammed P. K., Parameswaranpillai J., Thomas S.: Experiments and modeling of non-linear viscoelastic responses in natural rubber and chlorobutyl rubber nanocomposites. Applied Clay Science, **123**, 1–10 (2016). https://doi.org/10.1016/j.clay.2016.01.004

[46] Fu W., Wang L., Huang J., Liu C., Peng W., Xiao H., Li S.: Mechanical properties and mullins effect in natural rubber reinforced by grafted carbon black. Advances in Polymer Technology, **2019**, 4523696 (2019). https://doi.org/10.1155/2019/4523696